Detection and gradation of oriented texture

B.B. Chaudhuri, Pulak Kundu and Nirupam Sarkar

Electronics and Communication Sciences Unit, Indian Statistical Institute, 203 B.T. Road, Calcutta 700 035, India

Received 20 February 1992
Revised 12 June 1992

Abstract

Chaudhuri, B.B., P. Kundu and N. Sarkar, Detection and gradation of oriented texture, Pattern Recognition Letters 14 (1993) 147–153.

It is difficult to analyze oriented textures by conventional statistical or structural methods. This letter describes an approach to characterize texture orientation. The approach is based on directional evidence accumulation as in the Hough Transform. Also, a measure to grade the directional image is defined. Illustrative examples are presented to demonstrate the efficiency of the approach.

Keywords. Texture analysis, directional texture, Hough transform, degree of directionality.

1. Introduction

Textures which have a dominant local orientation everywhere, may be called *oriented textures.* Orientation is an important feature in computer-based recognition and description of objects as well as in the characterization of texture of a region. Analysis of orientation may be applied to practical problems such as detection of defects in wood and metal strips under bend and stress, regeneration of a missing portion in some texture field, etc. Continuous spatial orientation in texture is connected to the concepts of flow field and coherence which are considered to be intrinsic properties of images.

Techniques to analyze texture can be classified broadly into statistical and structural approaches. In statistical approaches, texture is considered to be a result of some random process, such as Markov random field, or fractal Brownian motion. In a structural approach, the texture is viewed as an irregular repetition of some primitive elements, called *texels.* Many oriented textures cannot be modelled easily by statistical or structural approaches and hence need special attention.

The reason of our ability to detect orientation has been understood from the discovery due to Hubel and Wiesel (1962) that the mammalian visual cortex contains orientation selective cells. Physiological study of orientation selective mechanism (Schiller et al. (1976)) and psychological study of oriented pattern perception (Glass (1969)) are reported in the literature. About the computational aspects of orientation, Zucker (1983) reported an approach based on the combination of outputs of several linear operators. Kanatani (1984) used integral geometry to determine surface orientation from the intersection of scan lines with the textures curves. Bajcsy (1972, 1973) used Fourier power spectra to detect texture direc-

Correspondence to: Prof. B.B. Chaudhuri, Electronics and Communication Sciences Unit, Indian Statistical Institute, 203 B.T. Road, Calcutta 700 035, India. Email: ncst.ernet.in!kbcscal!bbc

tionality. An interesting work is due to Strassman (1986) who analyzed the style or texture of brush strokes in Japanese paintings in order to create a realistic computer paintbrush. Kass and Witkin (1987) described an algorithm for orientation detection that is based on a direction-dependent bandpass filter the frequency response of which is defined as

$$F(r,\theta)=[\mathrm{e}^{-r^2\sigma_1^2}-\mathrm{e}^{-r^2\sigma_2^2}]2\pi \mathrm{i} r\cos\theta.$$

The passband is determined by the values of σ_1 and σ_2. According to the authors, good filter response is obtained if the ratios of sigmas lie in the range of 2–10. The orientation specificity is provided by the cosine dependence of the filter on θ. Rao (1990), on the other hand, finds gradients of the Gaussian smoothed image and computes a weighted average of the corresponding orientation estimates over a neighborhood. Kass and Witkin as well as Rao define a coherence measure that represents the degree of flow-like texture in the neighborhood.

An alternative and simple method of orientation detection based on evidence accumulation as in the Hough (1962) transform is proposed here. In this method, the edge image is formed by the Laplacian of Gaussian approach. An orientation histogram of dominant local orientation is created from the edge image. Next, the peaks and valleys of the orientation histogram are detected. The height and width of the peaks are used to define a measure of texture orientation. Illustrative examples on the Brodatz (1966) album textures are presented.

2. Detection of directionality

The directionality analysis is done here in three steps namely edge detection, directional histogram construction, and peak detection. Finally, a measure is proposed to grade the textures as strongly or weakly directional.

2.1. Edge detection

The edge image is formed from the gradient vector of magnitude G and angle ϕ with horizontal. Consider two masks (Bergholm (1988)):

$$h_x(i,j)=\frac{2i}{\sigma^2}\exp[-(i^2+j^2)/\sigma^2], \tag{1}$$

$$h_y(i,j)=\frac{2j}{\sigma^2}\exp[-(i^2+j^2)/\sigma^2] \tag{2}$$

where $-s<i,j<s$.

Determination of mask size s is a critical issue. A big mask needs more computation while a small mask can lead to inaccuracy. The mask size is chosen in such a way that the minimum magnitude of h_x or h_y at any point (i,j) except on the lines defined by $(0,j)$ and $(i,0)$ within the mask should be at least 0.01. The coordinates of the furthest points in the mask are $(\pm s, \pm s)$. At one of such points, say (s,s), the value of h_x is

$$h_x(s,s)=\frac{2s}{\sigma^2}\exp[-2s^2/\sigma^2]\geqslant 0.01.$$

Considering the minimum value of $h_x(s,s)$ we have

$$\frac{2s}{\sigma^2}\exp[-2s^2/\sigma^2]=0.01.$$

An approximate solution of this equation is given by (Bergholm (1988)):

$$s\approx\sigma\sqrt{-\log(0.005)-2\log\sigma}. \tag{3}$$

Note that at the points on the lines defined by $(0,j)$, h_x is zero while at the points on the line by $(i,0)$, h_y is zero.

These masks are convolved with the image I

$$G_x=(h_x*I),\qquad G_y=(h_y*I)$$

to get

$$G=(G_x^2+G_y^2)\quad\text{and}\quad \phi=\tan^{-1}[G_y/G_x]. \tag{4}$$

The gradient vector (G,ϕ) is computed on a mask of size $s\times s$ at each pixel of the image using equations (1)–(4). The resulting image can be called edge image E.

2.2. Dominant direction histogram construction

Let the direction be quantized at 1° interval. For an $m\times m$ pixel subimage W of the edge image E, an array of 180 accumulator bins are defined. Let A_θ^W denote the accumulator bin for edge contribution along direction θ.

The contribution of a pixel $(i,j) \in W$ in the accumulator A_θ^W is $G(i,j)\cos^2(\theta-\phi_{ij})$ where ϕ_{ij} is the angle of the gradient at (i,j). The contribution from all pixels can be written as

$$A_\theta^W = \sum_{(i,j)\in W} G(i,j)\cos^2(\theta-\phi_{ij});$$

$$0° \leqslant \theta < 180°. \tag{5}$$

An estimate of dominant direction in W is given by $\hat\theta$ so that

$$A_{\hat\theta}^W = \max_\theta A_\theta^W. \tag{6}$$

Another array, called *Histogram array* is used. The array consists of 180 elements, where element H_θ contains frequency for direction θ.

When a dominant direction $\hat\theta$ in a sub-image is detected by equation (6), $H_{\hat\theta}$ is incremented by 1,

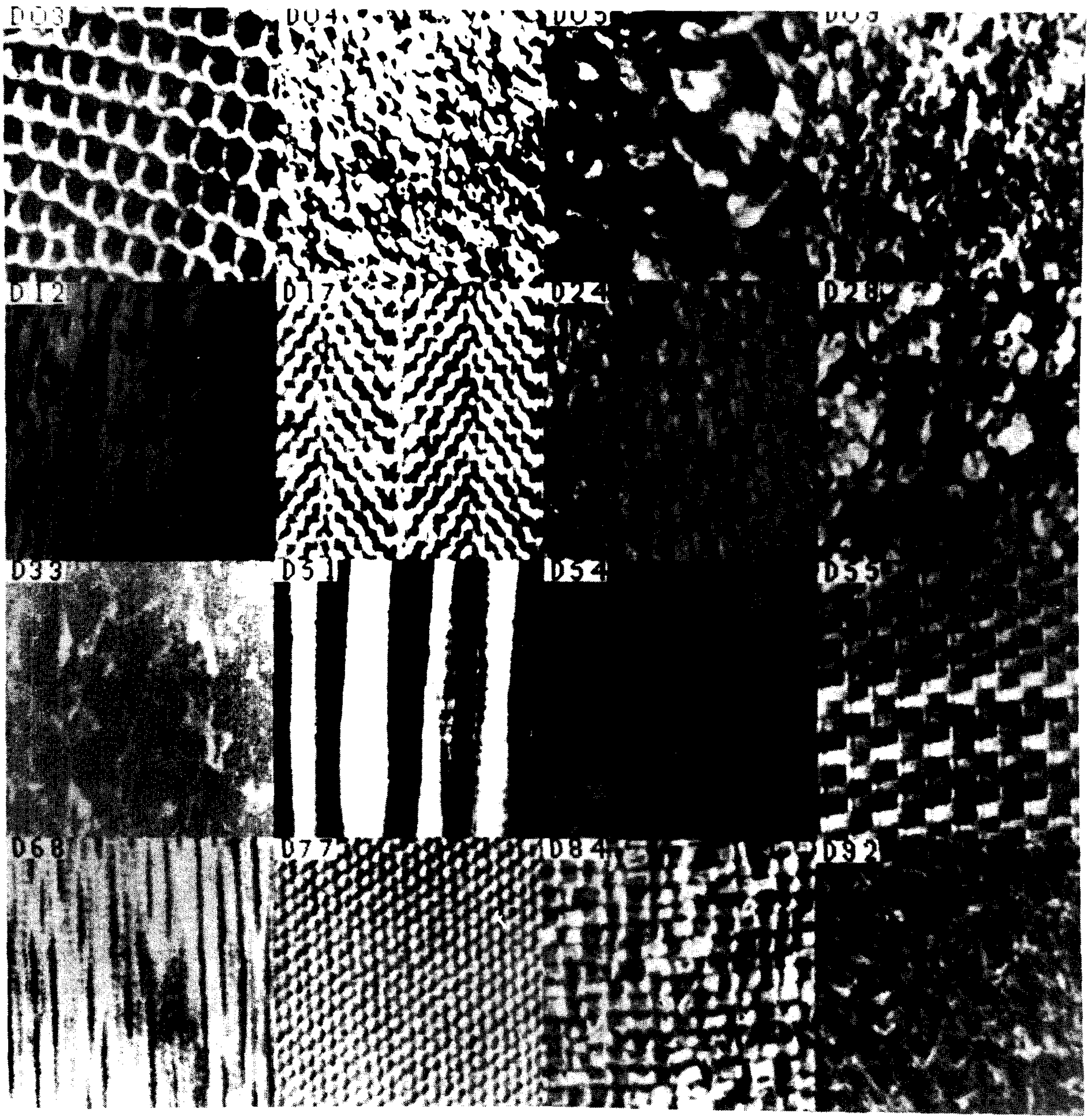

Figure 1. Texture images from Brodatz (1966) album.

i.e.,

$$H_{\theta} \longleftarrow H_{\theta}+1. \tag{7}$$

However, the plot of H_θ against θ often does not show a prominent peak even in strongly directional texture image. Hence, a modified histogram is generated by incrementing H_θ by μ, i.e.,

$$H_{\theta} \longleftarrow H_{\theta}+\mu \tag{8}$$

where

$$\mu=\frac{A_{\theta}^{W} \cdot 180}{\sum_{\theta} A_{\theta}^{W}}-1. \tag{9}$$

Note that μ is always positive since the first term on its right-hand side is always greater than 1. For directional textures, we have consistently found sharp peaks, whose positions have been detected by the following approach.

2.3. Peak detection

The histogram is smoothed by moving averaging to get rid of spurious peaks of high magnitudes. The window size used to compute moving average is 11. Although most of the spurious peaks are removed by the process, some unwanted peaks and valleys may still remain in the histogram. These peaks and valleys can be discarded by a simple thresholding approach. Let the average height of the histogram denote the threshold T_1, i.e.,

$$T_1=\sum_{\theta} H_{\theta}/180. \tag{10}$$

Then the following steps are taken:

Step 1. Choose the peaks above and valleys below the threshold (T_1). Discard any valley above and peak below the threshold T_1. If 'v' denotes a valley and 'p' denotes a peak, then the chosen extrema can be represented by a string of the type

vvvv ⋯ pppp ⋯ vvvv ⋯.

Step 2. From each cluster of peaks choose the one with maximum height. If N_p is the number of peak clusters, then N_p peaks are chosen in this way. Similarly, choose a valley from each cluster of valleys whose height is minimum. Now a sequence like vpvpvp ⋯ is formed. For the ith peak, say P_i, in this sequence, its immediate left neighbor valley position L_{v_i} and immediate right neighbor valley position R_{v_i} are detected. (If for the first peak a left valley is not detected then the histogram value at angle 0° is considerd as the left valley. Similarly, for the rightmost peak if a right valley is not detected then the histogram value corresponding to angle 179° is considered as the right valley.) Repeat till all N_p peaks are encountered.

Step 3. For each i find the span S_i corresponding to P_i as

$$S_i=R_{v_i}-L_{v_i}.$$

A measure of cut-off ratio of P_i can be defined as

$$f_{i1}=\frac{h_i-T_1}{h_i} \tag{11}$$

where h_i is the height of the ith peak P_i and T_1 is given by equation (10).

Also, a measure of sharpness of peak P_i can be defined as $f_{i2}=h_i/S_i$. From this measure some sort of gradation is made as follows:

$$Grade_i=\frac{f_{i2}}{1+f_{i2}}. \tag{12}$$

When the number of peaks is more than one, it may be useful to make an overall gradation of directionality. For two peaks with heights h_1, h_2 and widths S_1 and S_2, the overall gradation is proposed as

$$Grade_O=\frac{F}{1+F}, \quad \text{where } F=\frac{(h_1+h_2)}{(S_1+S_2)/2}. \tag{13}$$

The *'Grade'* is defined in such a way that it lies in [0, 1].

3. Results and discussion

To demonstrate the performance of our algorithm we took 16 texture images from the Brodatz (1966) album. They are shown in Figure 1. Each of these images is of size 128 × 128 and the image intensity is quantized into 256 gray levels. For each image, the edge image is computed using equations (1),(2) and (3) taking $\sigma=2.0$. For each edge image, accumulation (A_θ^W) is performed on

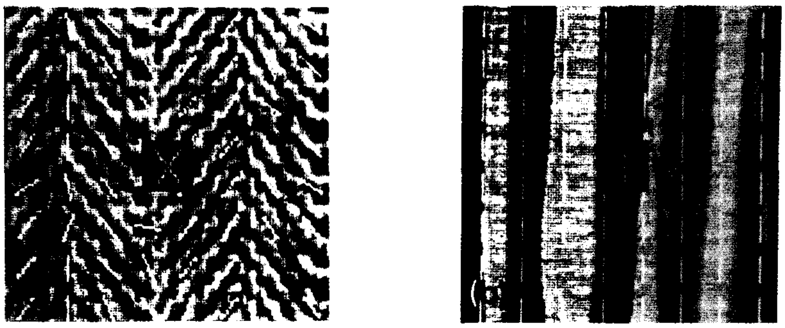

Figure 2. Strongly oriented texture images. (Local dominant directions are shown by white lines and Global dominant directions are shown by white line in black box.) (a) For D17, (b) for D51 of the Brodatz album.

each 12×12 overlapping window using equation (5), and the dominant direction in that window is found with help of equation (6).

It is to be noted that computation on overlapping windows results in a smoother histogram. 50% overlap in horizontal direction is used in our case. The additional computation requirement for the overlapping case can be reduced if the computation over the overlap region is memorized and used for two windows.

We considered Rao's approach to make a comparative study. In this approach, an edge image is formed in a similar manner as in Section 2.1. The direction to which the sum of projections of the edge vectors attains a maximum is considered as the best estimate for dominant local orientation. Let ϕ_{ij} be the angle that the gradient at pixel (i,j) makes in the $m\times m$ window W. The dominant orientation θ is given by

$$\theta=\frac{1}{2}\tan^{-1}\frac{\sum_{i=1}^{m}\sum_{j=1}^{m}G^2(i,j)\sin 2\phi_{ij}}{\sum_{i=1}^{m}\sum_{j=1}^{m}G^2(i,j)\cos 2\phi_{ij}}. \tag{14}$$

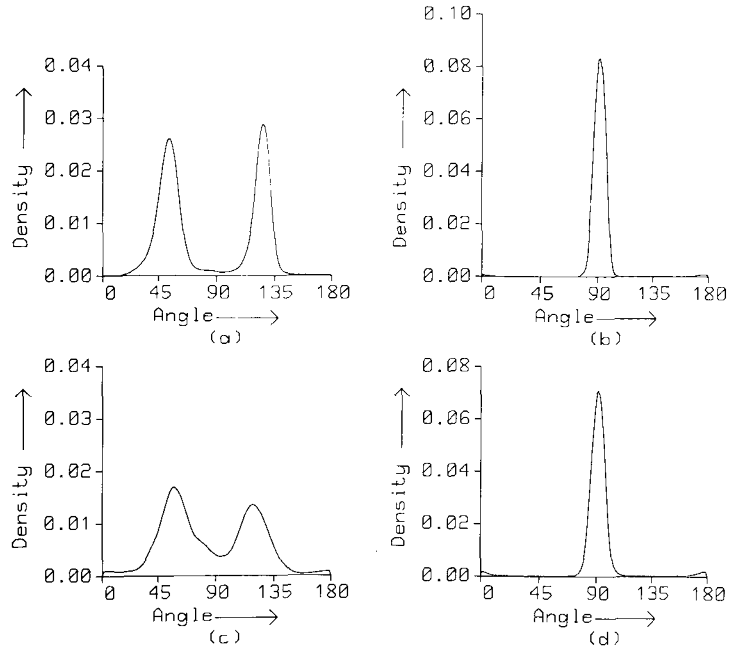

Figure 3. (a)-(b) Angle histogram of the image D17 and D51 respectively by the proposed method. (c)-(d) Angle histogram of the same images by Rao's (1990) method.

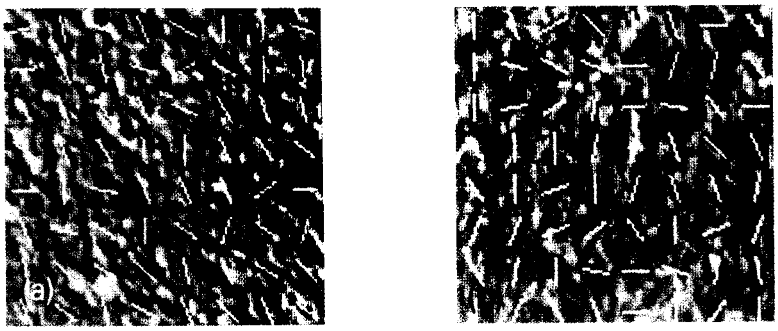

Figure 4. Weakly oriented texture images. (Local dominant directions are shown by white lines.) (a) For D04, (b) for D09 of the Brodatz album.

The oriented textures D17 and D51 and the local dominant directions are shown in Figure 2. The dominant direction histograms of these images D17 and D51 (from Figure 1) are shown in Figures 3(a) and 3(b), respectively. The density in these plots are obtained by normalizing the frequency $H_{\hat{\theta}}$ so that the area under the curve is unity. Comparatively, dominant direction histograms due to Rao's approach are shown in Figures 3(c) and 3(d) respectively. Some weakly oriented textures D04 and D09 and their local dominant directions are shown in Figure 4, while dominant direction histograms of the images are shown in Figures 5(a) and 5(b), respectively. Dominant direction histograms due to Rao's approach are shown in Figures 5(c) and 5(d) respectively.

Choice of window size is an important consideration since it affects the computational complexity and histogram shape. It has been seen that a small window size normally results in flat histograms. With increase in window size, the dominant peaks become more prominent till the process saturates. Larger window sizes, on the other hand, require more computation. For the

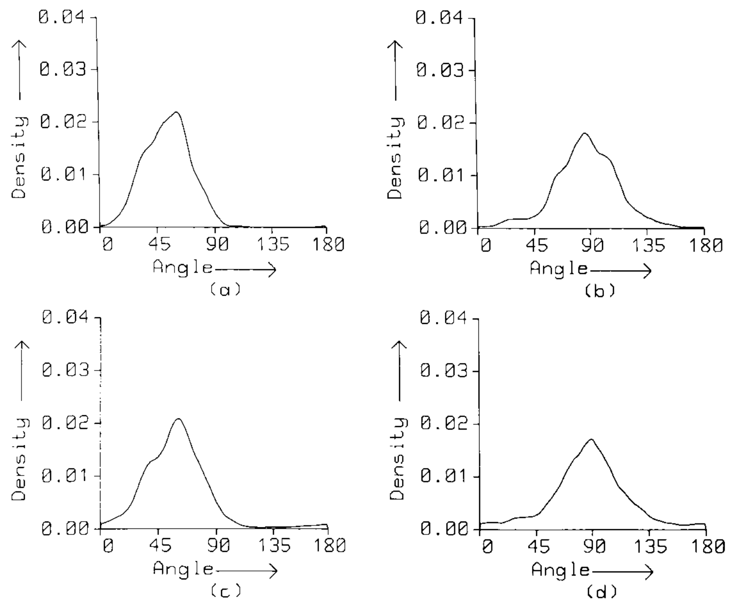

Figure 5. (a)–(b) Angle histogram of the images D04 and D09 respectively by the proposed method. (c)–(d) Angle histogram of the same images by Rao's (1990) method.

Table 1
Local dominant direction(s) and texture gradation

Image	# peaks	Angle	f_1	f_2	*Grade*	*Grade*$_0$
D03	2	41	0.500	4.629	0.177	0.446
		98	0.733	1.330	0.429	
D04	1	61	0.747	2.502	0.285	
D05	1	50	0.401	8.827	0.102	
D09	1	87	0.695	4.389	0.185	
D12	1	97	0.851	0.499	0.667	
D17	2	53	0.787	0.569	0.637	0.797
		126	0.807	0.455	0.688	
D24	1	85	0.838	0.689	0.592	
D28	1	101	0.714	3.018	0.249	
D33	1	99	0.667	2.511	0.285	
D51	1	92	0.933	0.079	0.927	
D54	0	–	–	–	–	
D55	1	163	0.858	0.688	0.592	
D68	1	88	0.932	0.087	0.920	
D77	1	115	0.889	0.402	0.713	
D84	2	94	0.761	1.224	0.449	0.464
		163	0.402	5.040	0.165	
D92	1	69	0.562	3.917	0.203	

current set of pictures, 12×12 windows are approximately optimum.

Dominant peaks of the histogram are considered as global orientation of the texture. The global orientations are shown inset in the figures of the textures of Figure 2. They conform to our visual notion of global orientation. It has been noted that the number of such orientations should not exceed two, since our capability of detecting three or more global orientations is poor. To suppress the display of irrelevant global peaks a threshold on f_{i1} is considered. Peaks P_i for which $f_{i1} < 1/3$ are discarded. As a result, the number of peaks did not exceed two in all of our experiments.

The feature f_{i2} is considered to test the sharpness of the dominant peak and the texture is graded using the measures in equations (12)–(13). The results are shown in Table 1. It is seen that the measure is high for strongly oriented texture and low otherwise. We can use the information to decide whether the conventional statistical or structural approach should be applied to the current texture under study.

Acknowledgements

Interest in the work by Prof. D. Dutta Majumder is acknowledged with thanks. The authors also wish to thank Prof. A.K. Jain of Michigan State University and Dr. B.M. Mehtre for supplying the texture images.

References

Bajcsy, R. (1972). Computer identification of textured visual scenes. A.I. Lab., Stanford Univ., Palo Alto, CA, Memo. AIM-180.

Bajcsy, R. (1973). Computer description of textured surface. *Proc. 3rd Int. Joint Conf. Artificial Intelligence*, 572–579.

Bergholm, F. (1988). Detection of edges and busy regions using Canny's edge detection. TRITA-NA-E8472, Royal Institute of Technology, Stockholm, Sweden.

Brodatz, P. (1966). *Texture: A Photographic Album for Artists and Designers*. Dover, New York.

Glass, L. (1969). Moire effect from random dots. *Nature* 243, 578–580.

Hough, P.V.C. (1962). A method and means for recognizing complex patterns. US Patent 3,069,654.

Hubel, D.H. and T.N. Wiesel (1962). Receptive fields, binocular interaction and functional architecture in the cats visual cortex. *J. Physiol.* 166, 106–154.

Kanatani, K.I. (1984). Detection of surface orientation and motion texture by a stereological technique. *Artificial Intelligence* 23, 213–237.

Kass, M. and A. Witkin (1987). Analyzing oriented patterns. *Computer Vision, Graphics and Image Processing* 37, 362–385.

Rao, A. (1990). *A Taxonomy for Texture Description and Identification*. Springer, New York.

Schiller, P.H., B.L. Finlay and S.F. Volman (1976). Quantitative studies of single-cell properties in monkey striate cortex II. Orientation specificity and ocular dominance. *J. Neurophysiol.* 39, 1320–1333.

Strassmann, S. (1986). Hairy brushes. *Computer Graphics* 20, 225–232.

Zucker, S. (1983). Computational and psychophysical experiments in grouping. In: J. Beck, B. Hope and A. Rosenfeld, Eds., *Human and Machine Vision*. Academic Press, New York.